Constraining black hole spin in PG 1535+547 amidst complex multi-layered absorption

Athulya Madathil-Pottayil
Dom Walton

Reflection Spectroscopy

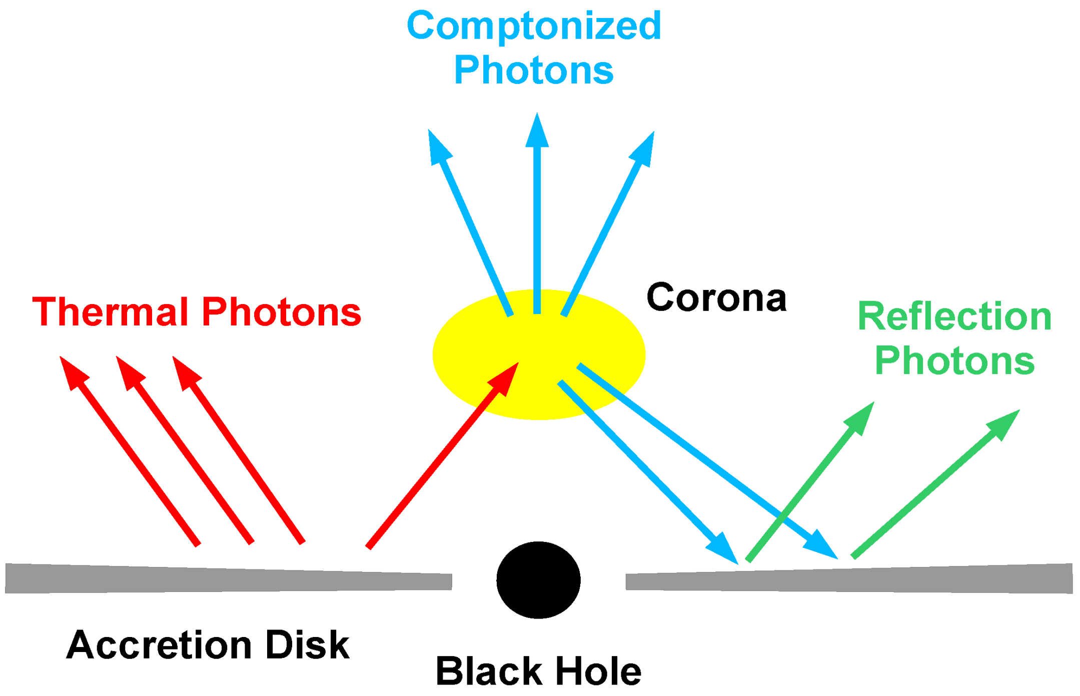

Bambi+23

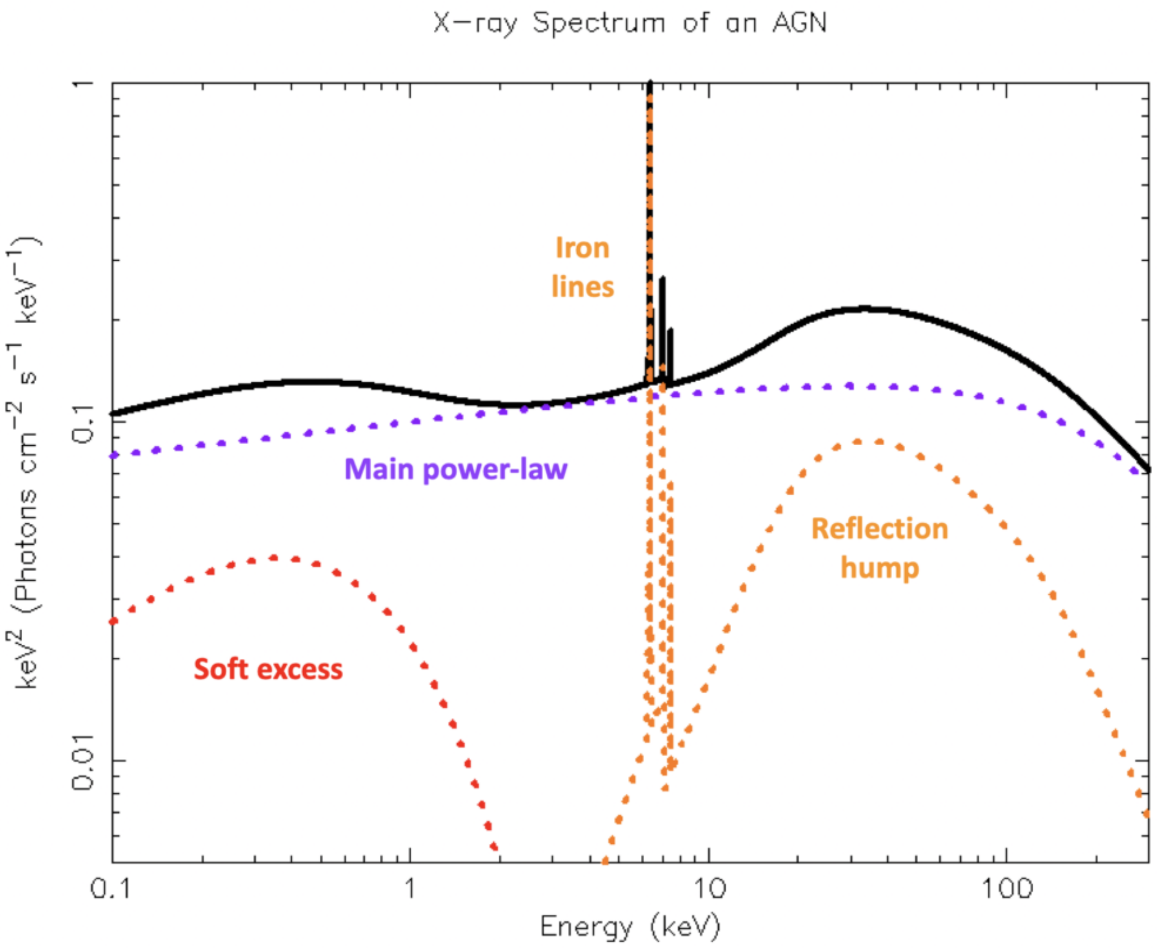

Reflection spectroscopy

Location & Geometry of the X-ray source

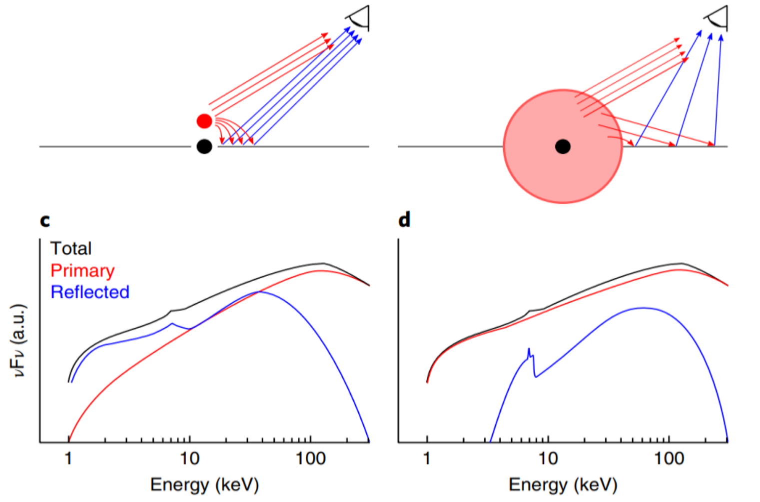

Chauvin+18

Properties of the accretion disc

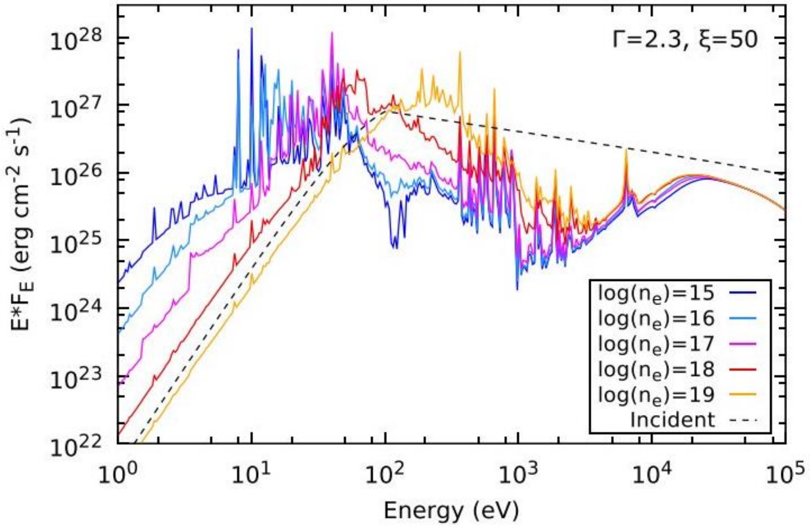

García+16

Spin of the black hole

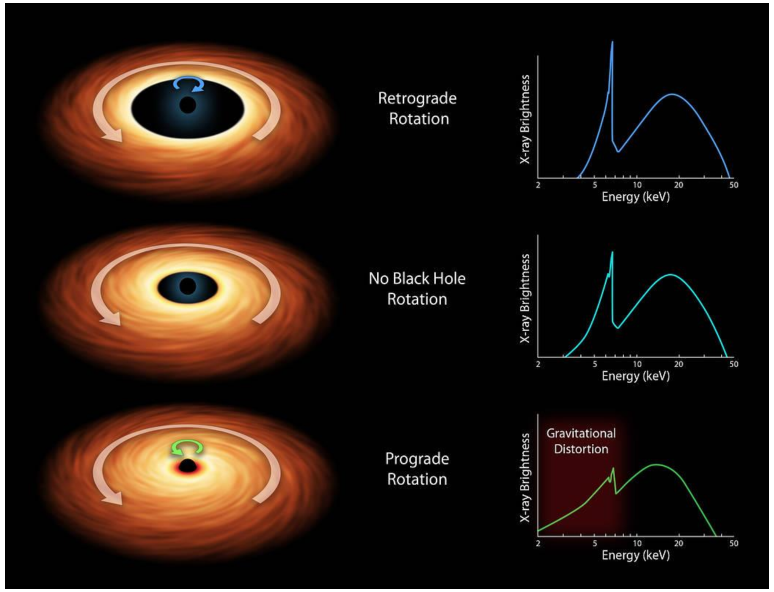

PG 1535+547 (a.k.a Mrk 486)

- Type I, radio-quiet AGN from the Palomar-Green Bright Quasar Survey (Schmidt & Green 1983)
- Black hole mass: ~1.5 × 10^7 $M_\odot$ (Hu et al. 2021)
- X-ray Observations from:
  - 2002 (*XMM-Newton*)
  - 2006 (*XMM-Newton*)
  - 2016 (*XMM-Newton* + *NuSTAR*)
- Highly complex X-ray spectrum including clear changes in line-of-sight absorption (Schartel et al. 2005, Ballo et al. 2008)

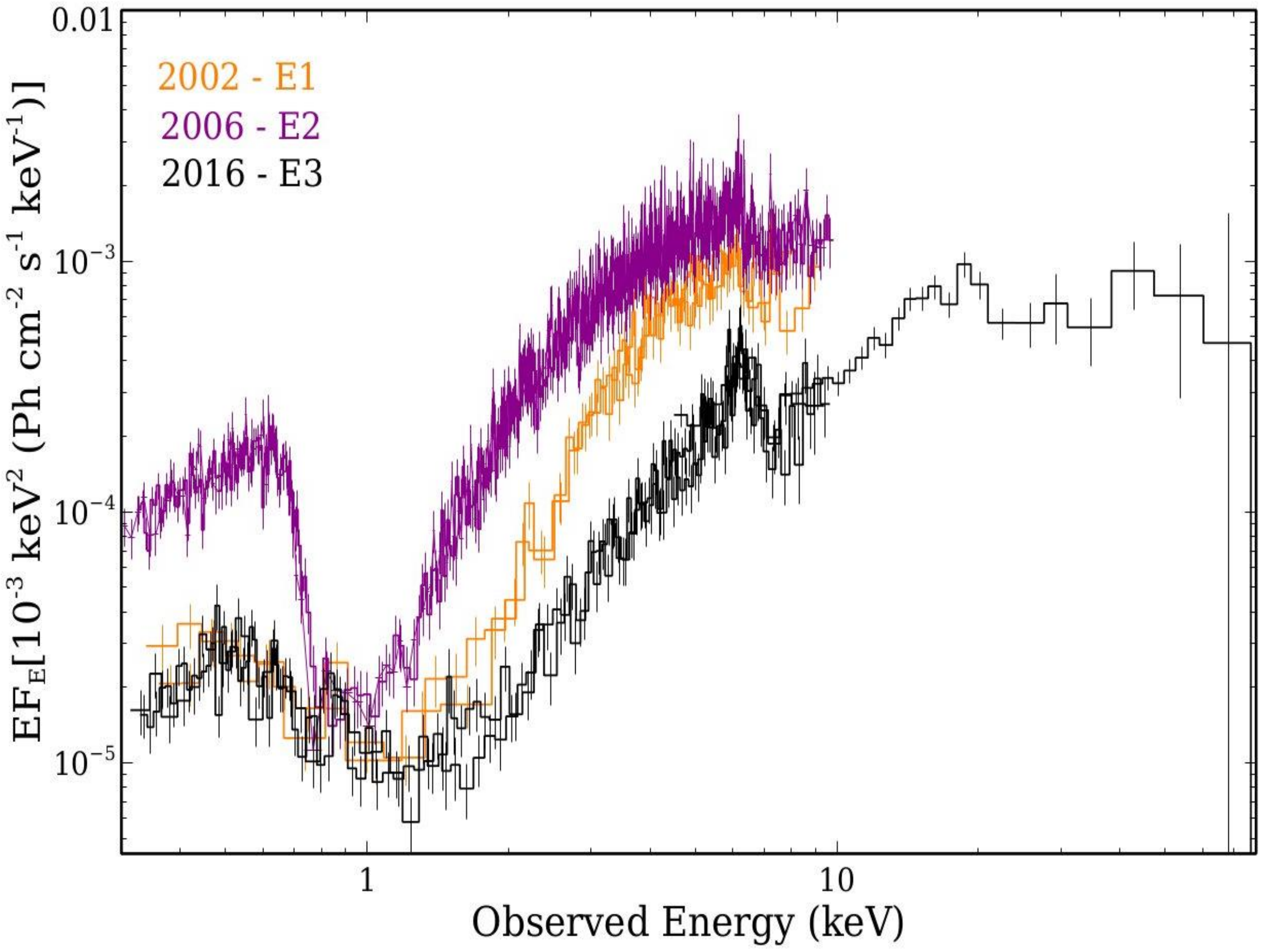

PG 1535+547 (a.k.a Mrk 486)

Emission features at ~ 6 – 7 keV

Compton hump at ~ 20 – 30 keV

Relativistic Reflection *(RELXILL)*

Significant variation at E < 3 keV

Epoch 2 : sharp edge ~ 0.7 keV

Warm absorbers *(Xstar)*

Flux variability across epochs 1, 2 & 3

Variation in spectral curvature > 2 keV

Warm absorption features undetected in 2002 and 2016 due to enhanced neutral obscuration

Variable Neutral obscuration *(Tbfeo)*

Steady flux at E < 1 keV

Diffuse plasma *(Mekal)*

Narrow iron line

Distant reflection *(Borus)*

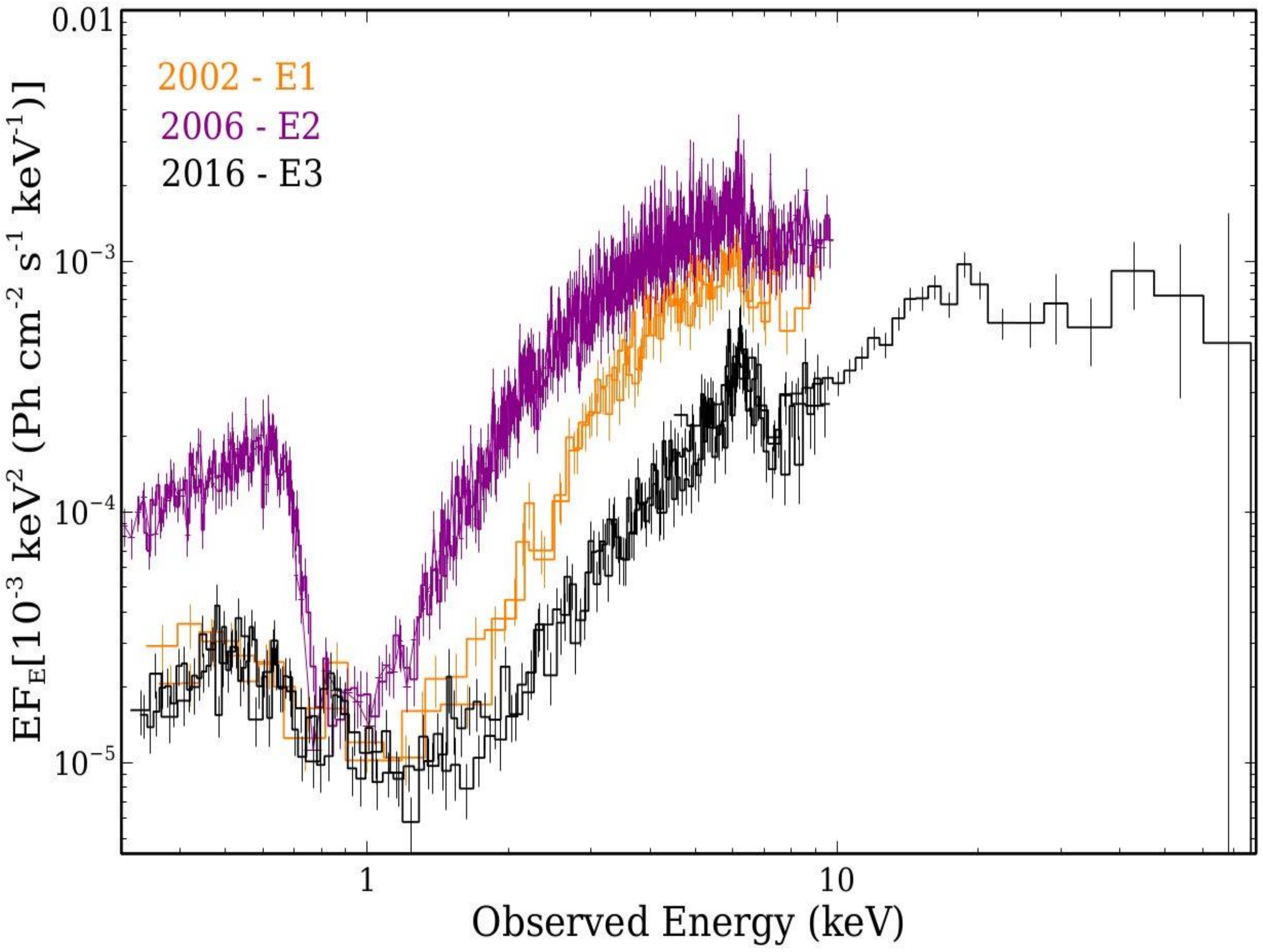

Multi-epoch Simultaneous spectral fit

relativistic reflection +
multiple layers of complex, time-dependent absorption along l.o.s

***ztbabs(powerlaw+mekal+borus+
(pcf ⊗ tbfeo) × (pcf ⊗ xstar$_1$) × xstar$_2$ × relxill(cp/lpcp)).***

- Observed variability cannot be solely attributed to l.o.s absorption changes
- Intrinsic continuum variability is also evident

Partially covering neutral absorber, during 2002 and 2016.
- 2002: $N_H \sim 3\times10^{22}$ cm^{-2}, *pcf* ~ 80%
- 2006: $N_H < 10^{20}$ cm^{-2}
- 2016: $N_H \sim 5\times10^{23}$ cm^{-2}, *pcf* ~ 50%

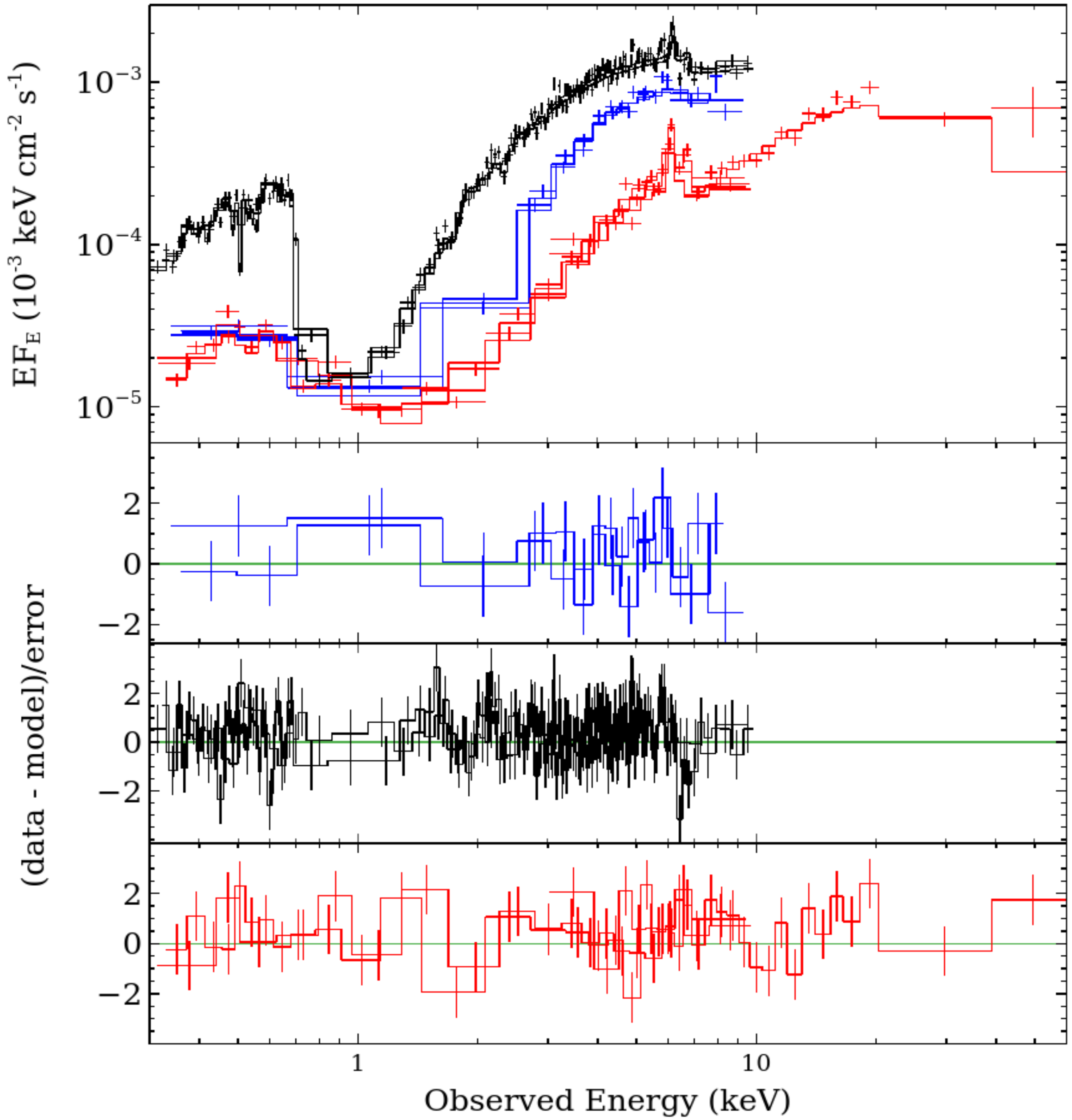

Light bending phenomenon in the reflection-dominated state

Epoch 1	*Epoch 2*
$\Gamma = 2.2 \pm 0.1$	$\Gamma = 2.2 \pm 0.1$
$h = 2.3\ (+7.4, -0.4)\ r_g$	$h = 6.8\ (+10.2, -2.1)\ r_g$
$R_{frac} = 2.9\ (+4.6, -2.2)$	$R_{frac} = 0.6\ (+0.3, -0.2)$

"Normal" reflection" , $R_{frac} \sim 1$, within errors,

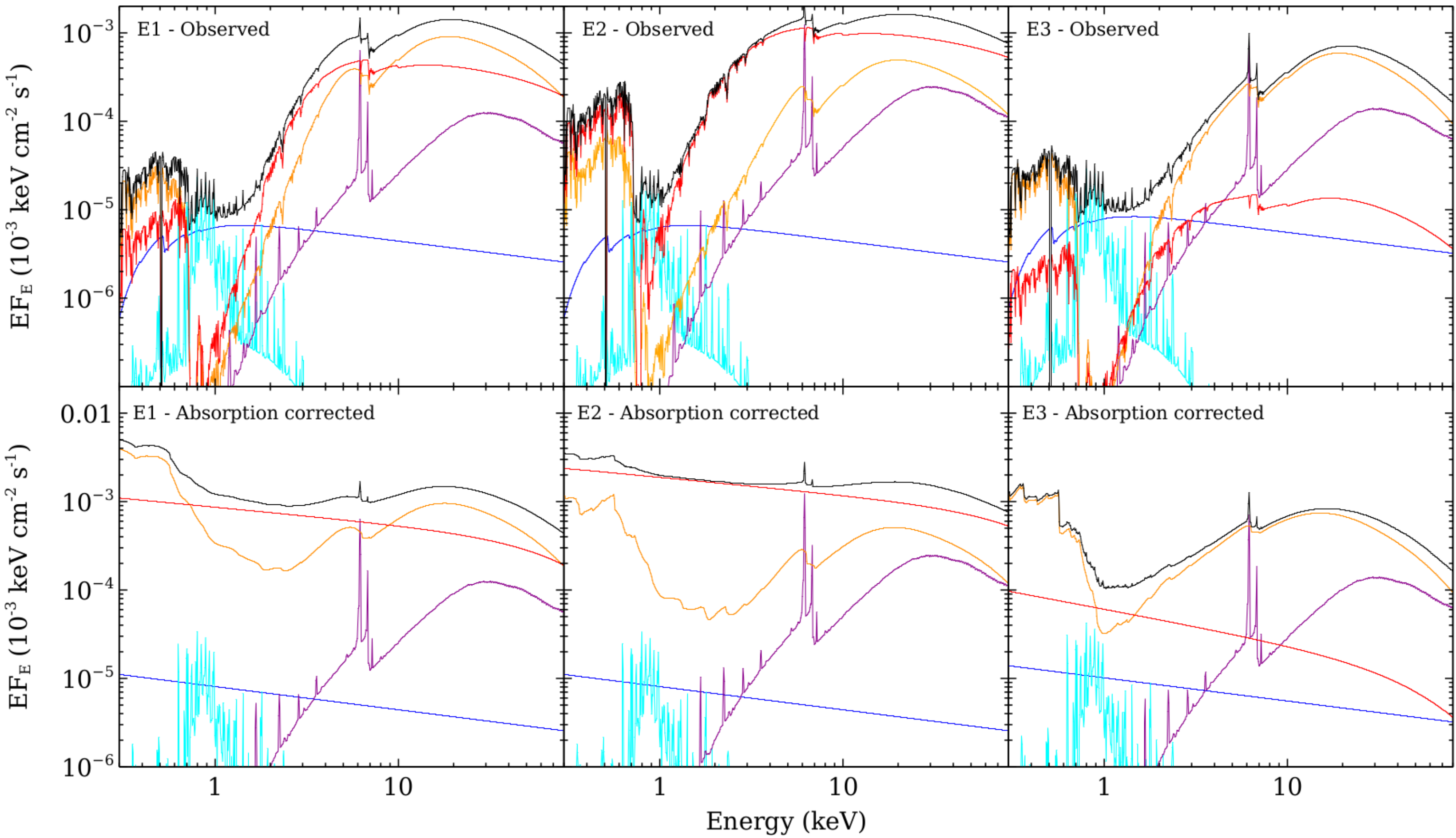

Epoch 3: Reflection-dominated state

- ***R_{frac}* > 7, *h* ≤ 1.72 rg.**
- **Intrinsic flux dropped × 7** in 2–10 keV band from 2006 to 2016
- **Variability** primarily driven by changes in **Comptonized intrinsic continuum**
- Similar Reflection-dominated states seen in IRAS 13224-3809, Mrk 335, MCG-06-50-15

- Consistent with "**light-bending**" (Miniutti & Fabian 2004): requires a **rapidly spinning** black hole and an **extremely compact x-ray source very close to the BH**

Spin of the black hole in PG 1535+547

- Spin constrained to a value of ***a** > 0.9** for PG 1535+547.

- Broadband **(*XMM* + *NuSTAR*)** data in 2016 **reflection-dominated state**, plus **joint 2002+2016 fit**, allowed spin constraints despite complex l.o.s. obscuration.

- A spin of $a^* > 0.9$ for $M_{BH} = 1.5 \times 10^7\ M_{\odot}$: a steady, radiatively-efficient accretion history for the black hole in PG 1535+547.

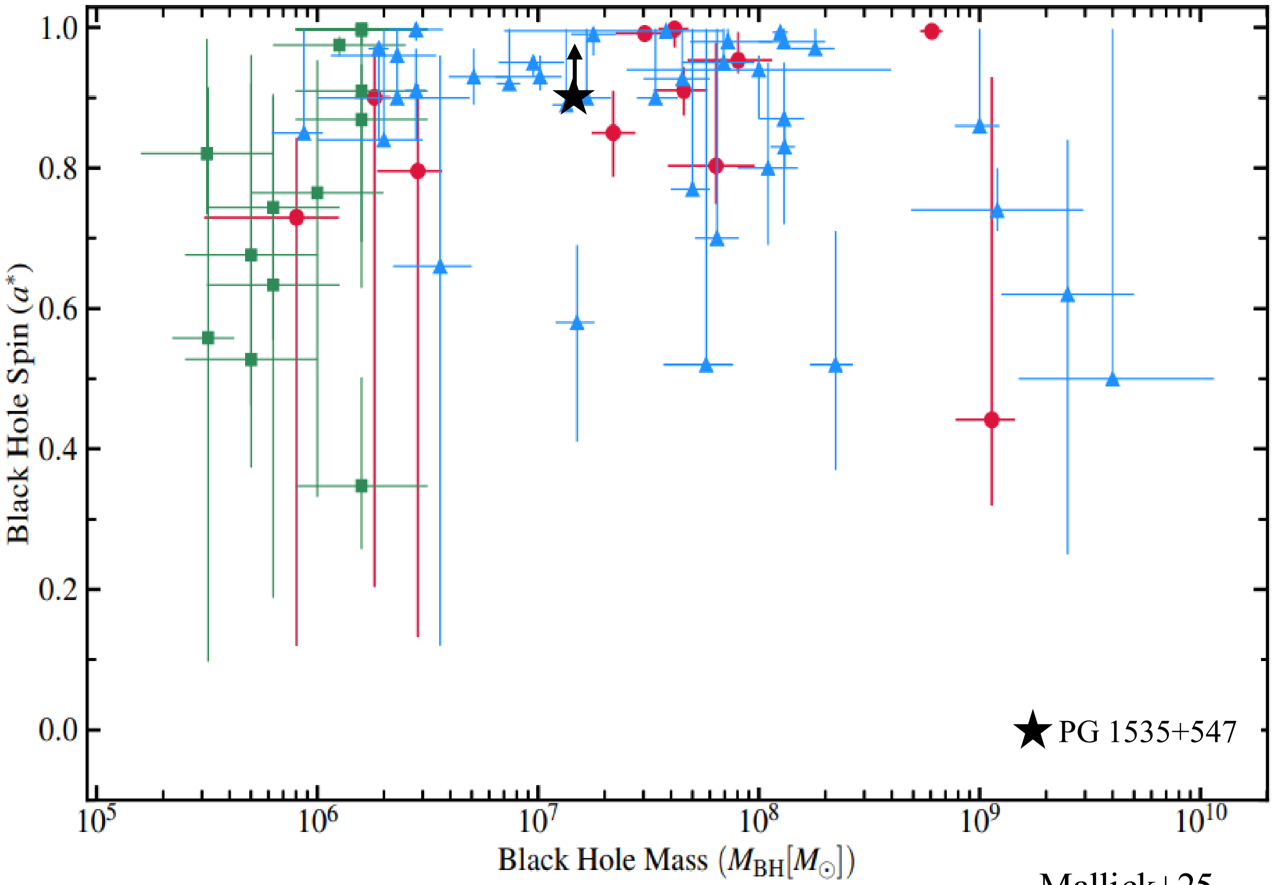

Mallick+25

Conclusions

PG 1535+547 exhibits strong spectral variability across all epochs.

Spectra explained by **relativistic reflection** + **multiple layers of complex absorption** along the line of sight.

Broadband *XMM* + *NuSTAR* coverage and **simultaneous multi-epoch fitting** enabled robust constraints, **despite complex obscuration**.

Primary continuum: $\Gamma \sim 2.2 - 2.4$

2016 : Reflection-dominated, with $\boldsymbol{R_{\mathrm{frac}} > 7}$, $\boldsymbol{h < 1.72\ r_g}$

- **Flux drop ×7**, consistent with **light-bending** scenario
- **Spin constraints:** Rapidly rotating black hole, $a^* > 0.9$

Neutral obscurer (partial): Detected in 2002 & 2016, $N_{\mathrm{H}} \sim 3 - 50 \times 10^{22}$ cm^{-2}, variable covering

log($M_{BH}\dot{m}^2$)-log(n_e) plane

- PG 1535+547 tested against the proposed anti-correlation between log($M_{BH}\dot{m}^2$)-log(n_e) in a radiation-pressure-dominated disc, as proposed by Svensson & Zdziarski (1994).
- For $\dot{m}$ = 1.05, log($M_{BH}\dot{m}^2$) ~ 7.2
- PG 1535+547 lies within the distribution the comparison sample of 31 Type I AGN.
- PG 1535+547 sits above 'f = 0.7', indicating that more than 70% of the disc's accretion power is dissipated into the corona.

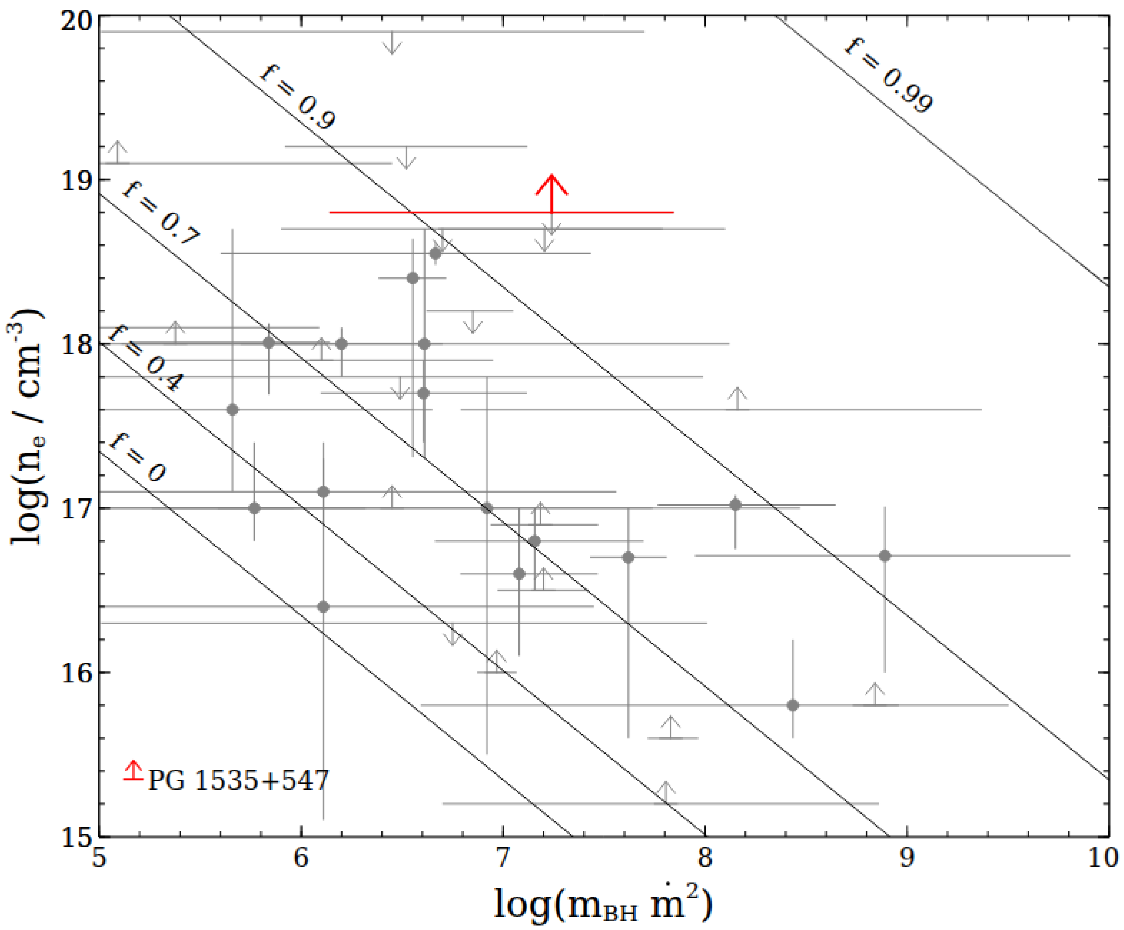

Table 1. Best-fitting parameters obtained from the simultaneous and the broad-band analysis of XMM–Newton + NuSTAR data of PG 1535 using the broken emissivity reflection model (relxillCP) and the lamppost models (relxilllpcp): *(zTBabs × TBabs(powerlaw + mekal + borus + (partcov ⊗ TBfeo) × xstar × (partcov ⊗ xstar) × relxillCp/relxilllpcp))*. All errors are quoted at 90% confidence level.

Model	Parameters	2002		2006		2016	
		relxillCP	relxilllpcp	relxillCP	relxilllpcp	relxillCP	relxilllpcp
ztbabs	N_H ($\times 10^{22}$cm^{-2})	$0.10^{+0.01}_{-0.01}$	$0.09^{+0.01}_{-0.01}$	$= ztbabs_{2002}$		$= ztbabs_{2002}$	
scattered PL	Norm ($\times 10^{-6}$)	$5.77^{+1.16}_{-1.66}$	$7.75^{+1.03}_{-1.54}$	$= scPL_{2002}$		$= scPL_{2002}$	
mekal	kT_e (keV)	$0.57^{+0.05}_{-0.05}$	$0.69^{+0.05}_{-0.06}$	$= mekal_{2002}$		$= mekal_{2002}$	
	Norm ($\times 10^{-6}$)	$0.41^{+0.08}_{-0.08}$	$1.17^{+0.26}_{-10.24}$				
Borus	log N_H (cm^{-2})	> 24.29	> 23.21	$= Borus_{2002}$		$= Borus_{2002}$	
	C factor	0.72	0.86				
partcov	pcf	$0.85^{+0.04}_{-0.08}$	$0.85^{+0.07}_{-0.07}$	-	-	$0.59^{+0.04}_{-0.23}$	$0.50^{+0.13}_{-0.07}$
tbfeo	N_H ($\times 10^{22}$cm^{-2})	$6.79^{+1.20}_{-1.69}$	$2.14^{+1.02}_{-0.64}$	-	-	$30.56^{+14.26}_{-10.93}$	$55.55^{+29.00}_{-17.24}$
xstar	N_H ($\times 10^{22}$cm^{-2})	$3.98^{+1.49}_{-0.74}$	$2.53^{+0.08}_{-0.29}$	$= xstar_{2002}$		$= xstar_{2002}$	
	log ξ (erg cm s^{-1})	$1.80^{+0.01}_{-0.02}$	$1.80^{+0.02}_{-0.01}$				
	A_O (solar)	$1.95^{+0.66}_{-0.11}$	$3.16^{+0.17}_{-0.10}$				
	z	$0.030^{+0.007}_{-0.008}$	$0.020^{+0.003}_{-0.005}$				
partcov	cvr.fr.	$0.79^{+0.02}_{-0.02}$	$0.80^{+0.02}_{-0.01}$	$= partcov_{2002}$		$= partcov_{2002}$	
xstar	N_H ($\times 10^{22}$cm^{-2})	$5.93^{+3.68}_{-1.13}$	$9.89^{+0.82}_{-0.14}$	$= xstar_{2002}$		$= xstar_{2002}$	
	log ξ (erg cm s^{-1})	< 0.90	$1.84^{+0.06}_{-0.07}$				
	z	> 0.027	> 0.033				
Reflection model	Γ	$2.23^{+0.15}_{-0.05}$ *	$2.21^{+0.08}_{-0.05}$ *	$2.23^{+0.15}_{-0.05}$ *	$2.21^{+0.08}_{-0.05}$ *	$1.90^{+0.08}_{-0.13}$	$2.40^{+0.04}_{-0.06}$
	log ξ (erg cm s^{-1})	$0.99^{+0.09}_{-0.48}$ *	$2.44^{+0.15}_{-0.20}$ *	$0.99^{+0.09}_{-0.48}$ *	$2.44^{+0.07}_{-0.06}$ *	$1.29^{+0.15}_{-0.18}$	< 0.69
	h (R_{ISCO})	-	$2.25^{+7.37}_{-0.36}$	-	< 1.72	-	$6.77^{+10.24}_{-2.10}$
	q_{in}	> 6.06	-	$4.12^{+1.29}_{-0.55}$	-	$6.30^{+1.70}_{-1.72}$	-
	R_{br} (R_{ISCO})	< 2.46	-	< 2.13	-	> 5.96	-
	R	$0.73^{+0.92}_{-0.52}$	$2.94^{+4.63}_{-2.17}$	$0.79^{+0.40}_{-0.36}$	$0.64^{+0.26}_{-0.25}$	> 4.39	> 7.24
	a^*	$0.942^{+0.047}_{-0.052}$	> 0.993				
	i (deg)	$41.72^{+4.90}_{-6.91}$	< 29.12				
	kT_e (keV)	$18.47^{+45.81}_{-6.23}$	> 52.64				
	log (n_e/cm^{-3})	> 18.81	$18.95^{+0.09}_{-0.13}$				
	A_{Fe} (solar)	$1.94^{+0.28}_{-0.28}$	$3.16^{+0.26}_{-0.19}$				
	Norm ($\times 10^{-5}$)	$2.38^{+0.23}_{-0.05}$	$13.5^{+7.63}_{-8.10}$	$2.09^{+0.43}_{-0.25}$	$4.46^{+0.26}_{-0.81}$	$0.21^{+0.20}_{-0.46}$	$9.74^{+3.35}_{-5.75}$
cflux	log(flux)	-	-				
χ^2/d.o.f		1275.4/1140	1272.5/1143				

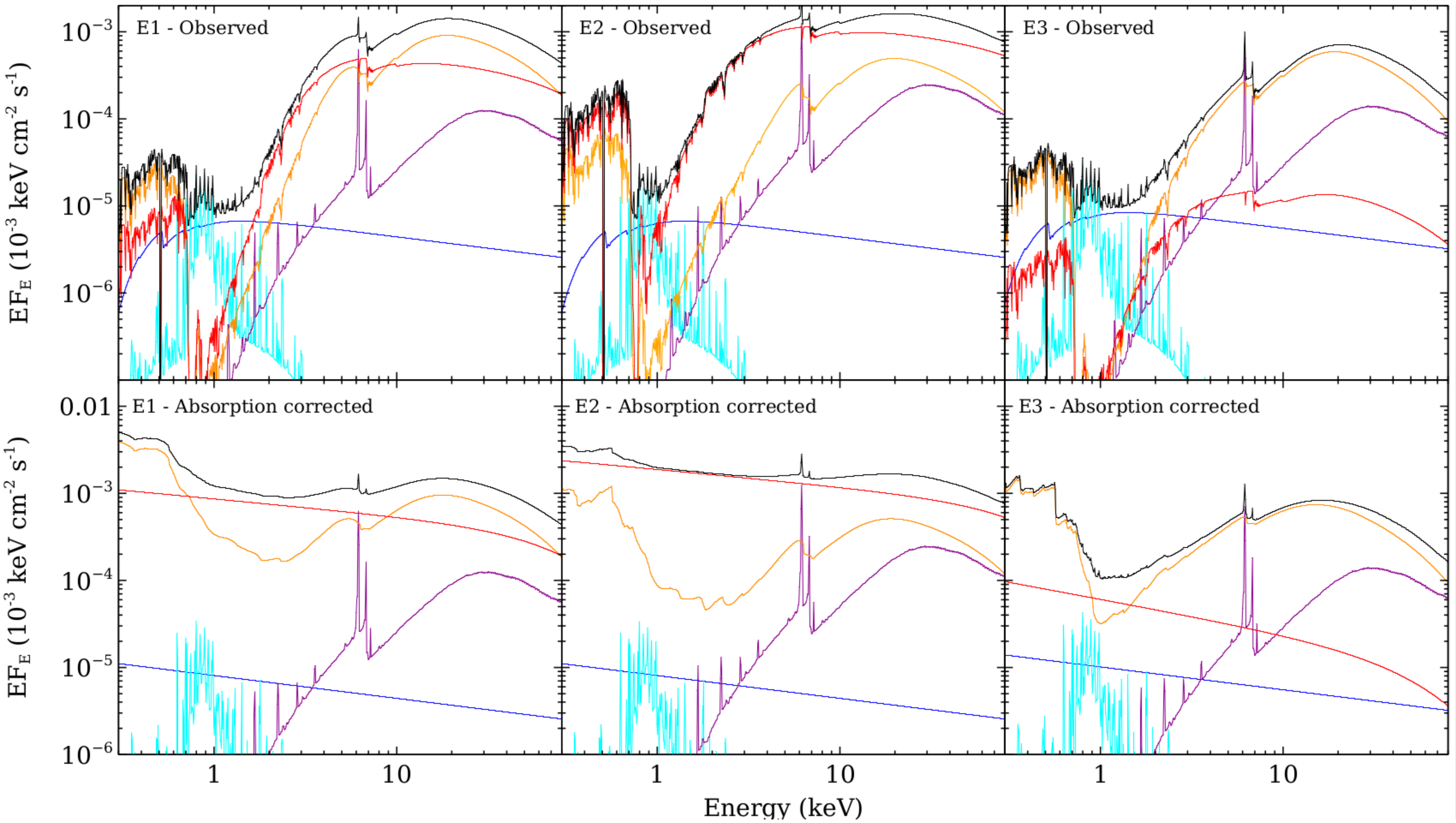
E1 - Observed
E2 - Observed
E3 - Observed
E1 - Absorption corrected
E2 - Absorption corrected
E3 - Absorption corrected
EF_E (10^{-3} keV cm^{-2} s^{-1})
EF_E (10^{-3} keV cm^{-2} s^{-1})
10^{-3}
10^{-4}
10^{-5}
10^{-6}
0.01
1
10
Energy (keV)

Warm Absorbers & Neutral Obscuration

- Complex, multi-layered absorption along the line-of-sight, characterized by
  - Partially covering Warm Absorber (WA_1)+
  - fully covering Warm Absorber (WA_2)
- $N_H(WA_1) \sim 1\times10^{23}$ cm^{-2}, log ξ (erg cm s^{-1}) ~ 1.8, *pcf* ~ 0.8, $v_{WA1} < 1450$ km s^{-1}
- $N_H(WA_2) \sim 3\times10^{22}$ cm^{-2}, similar ionization state to WA_1, $v_{WA2} \sim 5000$ km s^{-1}

- Partially covering neutral absorber, during 2002 and 2016.
  - 2002: $N_H \sim 3\times10^{22}$ cm^{-2}, *pcf* ~ 80%
  - 2016: $N_H \sim 5\times10^{23}$ cm^{-2}, *pcf* ~ 80%